PRAMANA
— journal of
physics

Vol. 64, No. 6
June 2005
pp. 881–892

Wetting and phase separation at surfaces

SANJAY PURI[1] and KURT BINDER[2]
[1]School of Physical Sciences, Jawaharlal Nehru University, New Delhi 110 067, India
[2]Institut für Physik, Johannes-Gutenberg-Universität Mainz, 55099 Mainz, Germany
E-mail: puri@mail.jnu.ac.in

Abstract. We study the problem of *surface-directed spinodal decomposition*, viz., the dynamical interplay of wetting and phase separation at surfaces. In particular, we focus on the kinetics of wetting-layer growth in a semi-infinite geometry for arbitrary surface potentials and mixture compositions. We also present representative results for phase separation in confined geometries, e.g., cylindrical pores, thin films, etc.

Keywords. Wetting; surface-directed spinodal decomposition; confined geometry.

PACS Nos 64.75.+g; 68.08.Bc

1. Introduction

A homogeneous binary (AB) mixture becomes thermodynamically unstable when it is rapidly quenched below the coexistence curve. The subsequent evolution of the system is characterized by the emergence and growth of domains enriched in either A or B. There has been intense research interest in these problems of *domain growth* or *phase ordering kinetics* [1–3].

In many experimental situations, the segregating mixture is in contact with a surface which is preferentially wetted by one of the components (say A) of the mixture [4,5]. In this case, there is growth of a surface wetting layer in conjunction with phase separation. The kinetics of wetting, and the segregation kinetics near the wetting layer, has also received much attention [6–8]. This process is usually referred to as *surface-directed spinodal decomposition* (SDSD) or *surface-directed phase separation*, and is of great scientific and technological importance.

We have a long-standing theoretical interest in the problem of SDSD. Here, we review some of our results in this context. This paper is organized as follows. In §2, we discuss microscopic and coarse-grained models for SDSD. In §3, we present analytical and numerical results for the case of a semi-infinite geometry. In §4, we discuss phase separation in confined geometries, e.g., pores, thin films. Finally, §5 concludes this paper with a summary and discussion of our results.

2. Theoretical modeling of surface-directed spinodal decomposition

2.1 *Model Hamiltonian*

Consider an AB mixture in contact with a surface S. There are pair-wise interactions $-E_{ij}^{\alpha\beta}$ between species α and β at sites i and j. Introduce the local concentration variables, $n_i^\alpha = 1$ if site i is occupied by an α-atom, and 0 otherwise. The corresponding Hamiltonian for a system with N atoms is

$$\mathcal{H} = -\sum_{i>j=1}^{N}\sum_{\alpha,\beta} E_{ij}^{\alpha\beta} n_i^\alpha n_j^\beta + \sum_{i=1}^{N}\sum_{\alpha} V_\alpha(\vec{r}_i) n_i^\alpha, \tag{1}$$

where lattice sites exist only in the positive half-space ($z \geq 0$). In general, $E_{ij}^{\alpha\beta}$ depends separately on $\vec{r}_i, \vec{r}_j$. For example, different interactions occur if both sites i, j are in the surface layer [9]. In eq. (1), $V_{\rm A}(\vec{r}_i)$ and $V_{\rm B}(\vec{r}_i)$ are potentials on A or B atoms at site i due to the surface at $z = 0$. The relative strength of these potentials and the AB surface tension determines whether the surface is *completely wet* (CW) or *partially wet* (PW) in equilibrium.

The correct description of microscopic detail is not relevant here. We will use the Hamiltonian in eq. (1) to motivate reasonable coarse-grained models, whose validity is substantially greater than the 'derivation' suggests. Therefore, we simplify the Hamiltonian by assuming that there are only nearest-neighbor interactions. Further, these are taken to be independent of i and j, except when they both lie in the surface layer. The surface potential usually depends only on the distance from the surface. In experiments, one can have both short-ranged potentials [$V(z) \sim \delta(z)$ or $V(z) \sim \exp(-z/z_0)$] and long-ranged potentials [$V(z) \sim z^{-n}$]. There are significant differences between wetting by short- and long-ranged potentials [10].

The semi-infinite Ising Hamiltonian corresponding to eq. (1) is obtained by introducing the spin variables $S_i = 2n_i^{\rm A} - 1 = 1 - 2n_i^{\rm B}$ as follows:

$$\begin{aligned}\mathcal{H} = &-\sum_{\langle ij\rangle} J_{ij} S_i S_j - H\sum_{i=1}^{N} S_i - H_1 \sum_{i_z=0} S_i \\ &+ \sum_{i_z\neq 0} V(z_i) S_i + \mathcal{H}_0, \quad S_i = \pm 1,\end{aligned} \tag{2}$$

where $\langle ij\rangle$ denotes a sum over nearest-neighbor pairs. The subscript $i_z = 0$ denotes sites i lying in the surface layer, and $\mathcal{H}_0$ is a constant. The interaction J_{ij} is

$$\begin{aligned}J_{ij} = J &= \frac{E^{\rm AA} + E^{\rm BB} - 2E^{\rm AB}}{4}, \quad i \text{ or } j \text{ not in surface}, \\ &= J_s = \frac{E_s^{\rm AA} + E_s^{\rm BB} - 2E_s^{\rm AB}}{4}, \quad i, j \text{ both in surface},\end{aligned} \tag{3}$$

where the subscript s refers to the surface. The bulk 'magnetic field' H is

$$H = \frac{q}{4}\left(E^{\mathrm{AA}} - E^{\mathrm{BB}}\right), \tag{4}$$

where q is the coordination number of a site. It is irrelevant in a fixed-magnetization ensemble. For sites in the surface layer, the magnetic field (for a cubic lattice) is

$$H + H_1 = \frac{q-2}{4}\left(E_s^{\mathrm{AA}} - E_s^{\mathrm{BB}}\right) + \frac{1}{4}\left(E^{\mathrm{AA}} - E^{\mathrm{BB}}\right) - \frac{1}{2}\left[V_{\mathrm{A}}(0) - V_{\mathrm{B}}(0)\right]. \tag{5}$$

Finally, we identify the potential as $V(z_i) = [V_{\mathrm{A}}(z_i) - V_{\mathrm{B}}(z_i)]/2$. Notice that we have absorbed the potential contribution at the surface into the definition of H_1. The surface field H_1 and the potential term are responsible for both surface enrichment and wetting phenomena in mixtures [9–12]. The generalization of the Hamiltonian in eq. (2) to any other geometry is obvious. For example, in a $d = 2$ film of thickness D, the RHS of eq. (2) would contain additional terms arising from the introduction of a surface at $z = D$.

We conclude this discussion by formulating the free-energy functional corresponding to the Hamiltonian in eq. (2). We introduce the space-dependent order parameter $\psi(\vec{r}_i) = \langle S_i \rangle$. Then, the free energy can be obtained by identifying $\psi(\vec{r}_j) = \psi(\vec{r}_i + \vec{r}_j - \vec{r}_i)$, and Taylor-expanding around $\vec{r}_i$:

$$\begin{aligned}\mathcal{F}[\psi] = \mathcal{H} - TS \simeq & \int \mathrm{d}\vec{r}\left[-\frac{1}{2}k_{\mathrm{B}}(T_{\mathrm{c}}-T)\psi^2 + \frac{k_{\mathrm{B}}T}{12}\psi^4 + \frac{J}{2}(\vec{\nabla}\psi)^2 + V(z)\psi\right] \\ & + \int \mathrm{d}\vec{\rho}\left\{-\frac{1}{2}\left[(q-2)J_s + J - k_{\mathrm{B}}T\right]\psi(\vec{\rho},0)^2 - H_1\psi(\vec{\rho},0)\right. \\ & \left. + \frac{J_s}{2}[\vec{\nabla}_{\parallel}\psi(\vec{\rho},0)]^2 - \frac{J}{2}\psi(\vec{\rho},0)\left.\frac{\partial\psi}{\partial z}\right|_{z=0}\right\}. \end{aligned} \tag{6}$$

Here, we have identified $\vec{r} = (\vec{\rho}, z)$, where $\vec{\rho}$ are the coordinates parallel to the surface, and z is perpendicular to the surface. The first term on the RHS of eq. (6) corresponds to the usual bulk energy, supplemented by a surface potential term. The bulk critical temperature is identified as $k_{\mathrm{B}}T_{\mathrm{c}} = qJ$. The second term is the surface contribution. The term $\partial\psi/\partial z|_{z=0}$ appears because of the missing neighbors for $z < 0$. The expansion which results in eq. (6) is only justifiable near criticality, where the order-parameter amplitude is small. However, we will also use this coarse-grained free energy far from criticality, and show that it successfully describes experimental phenomenology.

2.2 *Coarse-grained dynamical model*

A microscopic model for SDSD is obtained by associating spin-exchange kinetics with the Ising Hamiltonian in eq. (2). However, the corresponding continuum

model is more amenable to theoretical analysis. Binder and Frisch [13] used a master-equation approach to obtain a coarse-grained equivalent of the kinetic Ising model for a delta-function surface potential. This approach was modified by Puri and Binder [14], who explicitly incorporated a no-flux boundary condition into the model. The Puri–Binder model was the first successful coarse-grained model for SDSD. Here, we motivate it directly from the free-energy functional in eq. (6).

The bulk order-parameter equation is obtained from the continuity equation for the composition field $\psi(\vec{r},t)$. The resultant model is

$$\begin{aligned}\frac{\partial}{\partial t}\psi(\vec{r},t) &= -\vec{\nabla}\cdot\vec{J}(\vec{r},t) \\ &= \vec{\nabla}\cdot\{D\vec{\nabla}\mu(\vec{r},t)+\vec{\theta}(\vec{r},t)\} = \vec{\nabla}\cdot\left\{D\vec{\nabla}\left(\frac{\delta\mathcal{F}}{\delta\psi}\right)+\vec{\theta}(\vec{r},t)\right\} \\ &= \vec{\nabla}\cdot\left\{D\vec{\nabla}\left[-k_{\rm B}(T_{\rm c}-T)\psi+\frac{k_{\rm B}T}{3}\psi^3-J\nabla^2\psi+V(z)\right]+\vec{\theta}\right\}. \end{aligned} \tag{7}$$

The quantities $\vec{J}$ and μ in eq. (7) denote the current and chemical-potential difference between A and B, respectively; and D is the diffusion coefficient. This model is known as the *Cahn–Hilliard–Cook* (CHC) equation or *Model B* [15]. The Gaussian noise term has zero average and obeys the fluctuation–dissipation relation:

$$\overline{\theta_i(\vec{r}\,',t')\theta_j(\vec{r}\,'',t'')} = 2Dk_{\rm B}T\delta_{ij}\delta(\vec{r}\,'-\vec{r}\,'')\delta(t'-t''). \tag{8}$$

The surface order parameter rapidly relaxes to its equilibrium value and is not conserved. We assume a nonconserved (or *Model A* [15]) kinetics for $\psi(\vec{\rho},0,t)$:

$$\begin{aligned}\lambda^{-1}\frac{\partial}{\partial t}\psi(\vec{\rho},0,t) &= -\frac{\delta\mathcal{F}}{\delta\psi(\vec{\rho},0,t)} \\ &= [(q-2)J_s+J-k_{\rm B}T]\psi+\frac{J}{2}\frac{\partial\psi}{\partial z}\bigg|_{z=0}+H_1, \end{aligned} \tag{9}$$

where λ^{-1} sets the time-scale. The lateral-diffusion term has been neglected as the order parameter rapidly homogenizes at the surface. Finally, we implement a no-flux condition at $z=0$, viz.,

$$0 = \left\{D\frac{\partial}{\partial z}\left[k_{\rm B}(T_{\rm c}-T)\psi-\frac{k_{\rm B}T}{3}\psi^3+J\nabla^2\psi-V(z)\right]-\theta_z\right\}_{z=0}. \tag{10}$$

We will subsequently present results obtained for $T<T_{\rm c}$ from a dimensionless version of this model, which is as follows [6,8]:

$$\frac{\partial}{\partial t}\psi(\vec{r},t) = \vec{\nabla}\cdot\left\{\vec{\nabla}\left[-\psi+\psi^3-\frac{1}{2}\nabla^2\psi+V(z)\right]+\vec{\theta}\right\}, \tag{11}$$

where

$$\overline{\theta_i(\vec{r}\,',t')\theta_j(\vec{r}\,'',t'')} = 2\epsilon\delta_{ij}\delta(\vec{r}\,'-\vec{r}\,'')\delta(t'-t''),$$

$$\epsilon = \frac{1}{3}\left(\frac{T_c}{T}-1\right)^{-2}\xi_b^{-d}, \tag{12}$$

$\xi_b(=[q\,(1-T/T_c)\,/2]^{-1/2})$ being the bulk correlation length. The dimensionless boundary conditions are

$$\tau_0\frac{\partial}{\partial t}\psi(\vec{\rho},0,t) = h_1 + g\psi + \gamma\frac{\partial\psi}{\partial z}\bigg|_{z=0}, \tag{13}$$

$$0 = \left\{\frac{\partial}{\partial z}\left[-\psi+\psi^3-\frac{1}{2}\nabla^2\psi+V(z)\right]+\theta_z\right\}_{z=0}, \tag{14}$$

where τ_0, h_1, g, γ are parameters. Equation (13) rapidly relaxes the surface value of the order parameter to its equilibrium value, and will be replaced by its static version ($\tau_0 = 0$) subsequently. In general, the potential and the parameters ϵ, h_1, g, γ determine the equilibrium phase diagram of the surface [6, 16, 17].

The above model describes the case where segregation is driven by diffusion. However, many experiments on SDSD involve fluid mixtures, where hydrodynamic effects play an important role [18]. As in the diffusive case, one can study microscopic models, e.g., molecular dynamics (MD) simulations of mixtures near surfaces. Alternatively, one can study coarse-grained models like *Model H* at a surface [19]. The boundary conditions on the order-parameter field are similar to those described above. However, these must be supplemented with boundary conditions on the velocity field, e.g., the velocity vanishes at the surface.

3. Analytical and numerical results

3.1 *Wetting for critical quenches ($\psi_0 = 0$)*

Next, we discuss the kinetics of wetting, and phase separation in the vicinity of the wetting layer. We have used the above model to study SDSD for a wide range of mixture compositions [20], and potentials [21]: $V(z) = -V_0, z \le 1; V(z) = -V_0/z^n, z > 1$. Here, the cut-off is chosen to avoid the singularity at $z = 0$. Such power-law potentials are common in the context of surface-molecule interactions, e.g., $n = \kappa - d$, with $\kappa = 6$ and 7 corresponds to cases with non-retarded and retarded van der Waals' interactions, respectively [22]. For simplicity, we focus on the case with $E^{AA} = E^{BB}$ and $E_s^{AA} = E_s^{BB}$ in eq. (5), so that $h_1 = -V(0) = V_0$.

Figure 1 shows a snapshot for a critical mixture (with average order parameter $\psi_0 = 0$) evolving from a disordered initial condition. The parameters are such that the surface (at $z = 0$) is completely wetted by the component A. The surface exhibits a layered morphology, i.e., wetting layer followed by depletion layer, etc. This morphology is time-dependent and propagates into the bulk. The RHS of

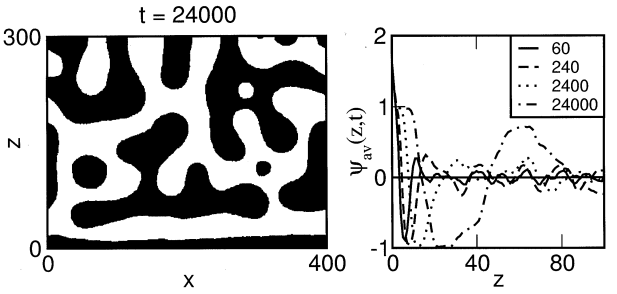

Figure 1. Snapshot at $t = 24000$ (frame on LHS) for an unstable AB mixture evolving from a disordered initial condition with $\psi_0 = 0$. The picture is obtained from an Euler-discretized version of eqs (11)–(14) (with $\Delta x = 1, \Delta t = 0.03$) on a $d = 2$ square lattice of size 400×300. The surface is at $z = 0$ and attracts A (with $\psi > 0$, marked in black) with a power-law potential $V(z) = -0.8/z^4$. The other parameters are $\tau_0 = 0, g = -0.4, \gamma = 0.4$, corresponding to complete wetting in equilibrium. The noise amplitude is $\epsilon = 0.041$, which corresponds to a deep quench with $T \simeq 0.22 T_c$. The frame on the RHS shows laterally averaged profiles at $t = 60, 240, 2400, 24000$ for this evolution.

figure 1 shows the laterally averaged profiles, $\psi_{\rm av}(z,t)$ vs. z, for the evolution. These are obtained by averaging $\psi(x,z,t)$ along the x-direction for a typical evolution, and also averaging over independent runs. This is the numerical counterpart of the lateral-averaging which yields experimental density-depth profiles [4, 5] – these are comparable to the RHS of figure 1. The averaging yields $\psi_{\rm av}(z,t) \simeq \psi_0 = 0$ in the bulk, where the phase-separation profiles are randomly oriented. However, a systematic behavior is seen at the surface. The wetting profiles are characterized by the zero-crossings of $\psi_{\rm av}(z,t) - \psi_0$. We denote the first and second zeros as $R_1(t)$ and $R_2(t)$, respectively, and will study them in detail here.

Apart from the wetting-layer kinetics, it is also relevant to quantify the nature of domain growth in the vicinity of the wetting layer. Puri *et al* [14, 21] have studied z-dependent correlation functions for a critical quench and a range of surface potentials. Their studies support the following picture. Domains near the wetting layer are characterized by two length scales $L_\parallel(z,t), L_\perp(z,t) \sim t^{1/3}$, with $L_\parallel > L_\perp$ (see figure 1). The length scale parallel to the surface is larger because of the orientational effect of the layered morphology at the surface. However, the enhancement is only in the prefactor of the growth law. Furthermore, these length scales cross over to diffusive growth ($L_\parallel(z,t) \sim t^{1/2}$) as the domains are absorbed into the wetting layer which propagates into the bulk.

Next, we develop a theory for the growth kinetics of the wetting layer. It is experimentally relevant to do this for mixtures with arbitrary composition. We first consider the case where the wetting component is the minority component.

3.2 *Wetting by the minority component* ($\psi_0 < 0$)

Figure 2 shows an evolution snapshot for SDSD with $\psi_0 = -0.4$, corresponding to a mixture with 30% A (the preferred component) and 70% B. The bulk (large z) is

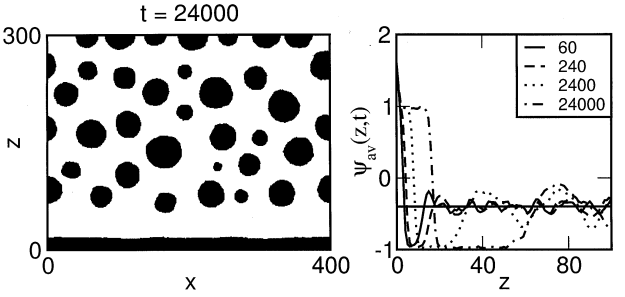

Figure 2. Analogous to figure 1, but for $\psi_0 = -0.4$.

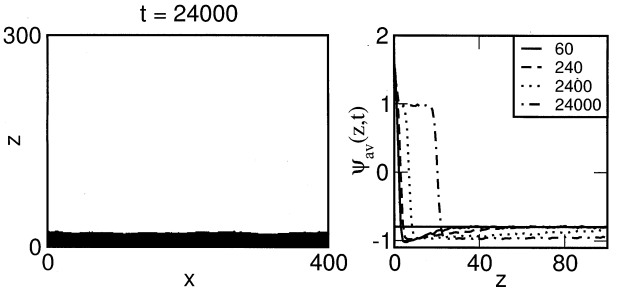

Figure 3. Analogous to figure 1, but for $\psi_0 = -0.8$.

characterized by the usual droplet morphology for off-critical phase separation [23]. As in figure 1, there is a wetting layer of the preferred component at the surface, which is followed by a depletion layer. The evolution of the laterally averaged profiles is shown on the RHS of figure 2.

Next, consider the evolution of an extremely off-critical case ($\psi_0 = -0.8$ or 10% A and 90% B) in figure 3. In this case, the thermal fluctuations are not sufficient to nucleate an A-rich droplet on the time-scale of our Langevin simulation. Thus, there is no bulk phase separation but there is a rapid growth of the wetting layer at the surface. The RHS of figure 3 shows the laterally averaged profiles. The behavior is qualitatively different from that for $\psi_0 = 0, -0.4$, due to the absence of bulk phase separation. The A-rich wetting layer is followed by a layer which is moderately depleted in A, and extends deep into the bulk.

First, consider the case where the bulk undergoes phase separation (as in figures 1 and 2). The thickness of the depletion layer is $h(t) = R_2(t) - R_1(t)$. The growth of the wetting layer is driven by two factors: (a) The surface-potential gradient drives A to the wetting layer with a current $-V'(R_1)$. (b) The intrinsic chemical potential μ (due to local curvature) is higher on the curved surface of bulk A-rich droplets than on the flat wetting layer. We have $\Delta\mu \sim \sigma/L$, where $L(t)$ is the bulk domain size, and σ is the surface tension. The corresponding current contribution at the wetting layer is $-\sigma/(Lh)$.

Thus the A-current in the z-direction is $J_z \simeq -V'(R_1) - \sigma/(Lh)$. To estimate $h(t)$ in terms of $R_1(t)$, we assume that the wetting and depletion layers have an overall composition of ψ_0. Then

$$R_2(t) \simeq \frac{2}{1+\psi_0} R_1(t), \quad h(t) \simeq \frac{1-\psi_0}{1+\psi_0} R_1(t). \tag{15}$$

The validity of eq. (15) has been confirmed by Puri and Binder [20].

For the case of a power-law potential, we have

$$\frac{\mathrm{d}R_1}{\mathrm{d}t} = -J_z \simeq \frac{nh_1}{R_1^{n+1}} + \frac{\sigma}{LR_1}\left(\frac{1+\psi_0}{1-\psi_0}\right). \tag{16}$$

The bulk length scale obeys the Lifshitz–Slyozov (LS) law $L(t) = f(\psi_0)(\sigma t)^{1/3}$, where $f(\psi_0)$ is known analytically for $|\psi_0| \to 1$ [1], but only numerically for other values of ψ_0 [23]. The first term on the RHS of eq. (16) is dominant at early times (for $n > 1$) and the second term is dominant at late times. Thus

$$\begin{aligned} R_1(t) &\sim (h_1 t)^{1/(n+2)}, \quad t \ll t_\mathrm{c}, \\ &\sim \sqrt{\frac{(1+\psi_0)}{f(\psi_0)(1-\psi_0)}}\,(\sigma t)^{1/3}, \quad t \gg t_\mathrm{c}. \end{aligned} \tag{17}$$

The cross-over between the potential-dependent growth regime and the universal regime ($R_1 \sim t^{1/3}$) can be extremely delayed, depending on the parameters and mixture composition. This explains the diverse growth exponents reported by various experiments and simulations. Figure 4a plots $\ln[R_1(t)]$ vs. $\ln t$ for $\psi_0 = 0, -0.2, -0.4, -0.6$ with $V(z) \sim z^{-4}$, and illustrates this cross-over behavior.

We separately discuss the cases of the power-law potential with $n = 1$; and the short-ranged potential $V(z) = -V_0 \exp(-z/z_0)$. For $V(z) \sim -z^{-1}$, both terms on the RHS of eq. (16) are comparable and the growth law is always the LS law, $R_1(t) \sim t^{1/3}$. On the other hand, the short-ranged potential yields a logarithmic early-time growth, $R_1(t) \sim z_0 \ln(h_1 t/z_0^2)$, which rapidly crosses over to the universal LS growth law. However, thermal fluctuations may interfere with the observation of the logarithmic growth regime [24].

Finally, consider the case of far-off-critical quenches ($\psi_0 \ll 0$), as in figure 3. Here, there are no bulk droplets to feed the wetting layer. Thus, the chemical potential in the bulk is the uniform value $\mu_0 = \psi_0^3 - \psi_0$. The current to the wetting layer is $-\mu_0/h$, where $h(t)$ is the scale on which the order parameter saturates to its bulk value (see figure 3). We neglect lateral fluctuations and assume a simple form (motivated by the solution of the linearized model [25]) for $\psi(z,t)$ as follows:

$$\begin{aligned} \psi(z,t) &\simeq 1, \quad z < R_1(t), \\ &\simeq \psi_0 - B_0 \mathrm{e}^{-(z-R_1)/h}, \quad z > R_1(t), \end{aligned} \tag{18}$$

where B_0 is a parameter. The composition constraint yields $h(t) \simeq (1-\psi_0)R_1(t)/B_0$. Thus, eq. (16) is modified as

$$\frac{\mathrm{d}R_1}{\mathrm{d}t} \simeq \frac{nh_1}{R_1^{n+1}} + \frac{\mu_0 B_0}{1-\psi_0}\frac{1}{R_1} = \frac{nh_1}{R_1^{n+1}} + \frac{|\psi_0|(1+\psi_0)B_0}{R_1}. \tag{19}$$

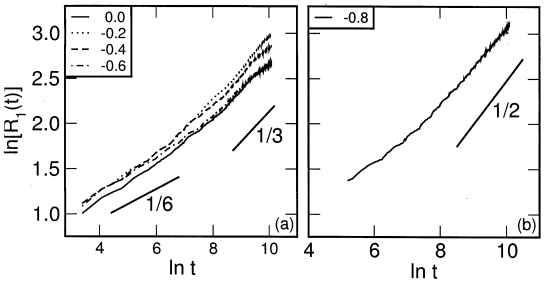

Figure 4. (**a**) Plot of $\ln[R_1(t)]$ vs. $\ln t$ for mixtures with $\psi_0 = 0, -0.2, -0.4, -0.6$. The straight lines have slopes 1/6 and 1/3, respectively. The exponent $\phi = 1/6$ corresponds to potential-dependent growth for the power-law potential with $n = 4$. (**b**) Plot of $\ln R_1$ vs. $\ln t$ for a far-off-critical case with $\psi_0 = -0.8$. The straight line has a slope of 1/2.

The corresponding growth regimes in this case are (for any value of n)

$$R_1(t) \sim (h_1 t)^{1/(n+2)}, \quad t \ll t_c,$$

$$\sim [|\psi_0|(1+\psi_0)B_0]^{1/2}\, t^{1/2}, \quad t \gg t_c. \tag{20}$$

Figure 4b shows data for $\ln[R_1(t)]$ vs. $\ln t$ for $\psi_0 = -0.8$, illustrating the asymptotically diffusive growth of the wetting layer. For a short-ranged surface potential, the initial growth regime is logarithmic, as before.

3.3 *Wetting by the majority component* ($\psi_0 > 0$)

We have also investigated the case with $\psi_0 > 0$, so that the majority component wets the surface. For brevity, we do not show detailed results here, and confine ourselves to a brief discussion of the coarsening scenario [20]. In this case, the bulk droplets are of the non-wetting component B. A thin wetting layer is formed and grows very slowly. The depletion layer that forms adjacent to the wetting layer is hardly apparent in this case.

It is somewhat counter-intuitive that the wetting layer grows so slowly when the majority component wets the surface. This is because the bulk droplets now compete with (rather than feed) the wetting layer for the preferred component A, as the intrinsic chemical potential for A is lower on the surface of the drops. Thus, the intrinsic chemical-potential gradient actually drives A into the bulk [20].

The far-off-critical case (with $\psi_0 \gg 0$) is analogous to surface enrichment kinetics seen for $T > T_c$ [25]. Of course, this assumes that there is no nucleation of droplets over extended time-scales. If droplets are nucleated, the scenario described above is applicable again.

4. Phase separation in a confined geometry

So far, we have described modeling and results for semi-infinite systems. The modeling of phase separation in confined geometries is a straightforward generalization.

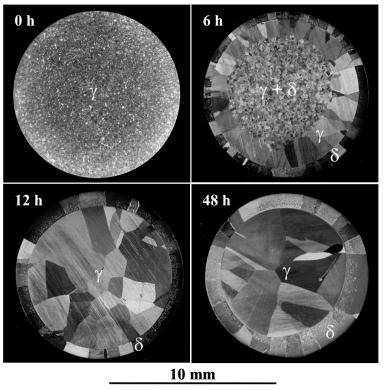

Figure 5. Phase-separation kinetics in cylindrical samples of steel mixtures of ferrite (δ) and austenite (γ) phases. The δ-phase wets the open surface.

Thus, for a thin film of thickness D, we impose the boundary conditions in eqs (13), (14) at $z = D$ with an appropriate surface potential [26]. The dynamical behavior is now much richer due to the interaction of SDSD waves originating from different surfaces. We discuss two recent works in this context.

4.1 *Experiments on SDSD in cylindrical samples of steel mixtures*

Aichmayer *et al* [27] have reported the first observation of SDSD in solid mixtures of ferrite (δ, bcc) and austenite (γ, fcc) stainless steels. These mixtures were prepared as cylindrical specimens with diameter 10 mm, and were quenched into the two-phase ($\delta + \gamma$) region of the phase diagram. The δ-phase is preferentially driven to the surface due to (a) the atmosphere around the samples; and (b) the presence of long-ranged strain fields. Figure 5 shows the evolution of the unstable mixture. An enriched layer of the ferrite phase forms at the surface, followed by a depletion layer and then the bulk region. This is analogous to figures 1 and 2. The SDSD profiles propagate into the bulk, resulting in a macroscopic segregated state, which is dictated by the composition of the mixture.

Aichmayer *et al* also undertook Langevin simulations of the SDSD model in eqs (11)–(14) in a cylindrical geometry. Their numerical results replicate the evolution seen in figure 5 at both the pictorial and quantitative levels.

4.2 *SDSD in a thin-film geometry*

In a recent work, Das *et al* [28] have undertaken Langevin and MD studies of phase separation of AB mixtures in thin films. They consider *symmetric* or *antisymmetric* films, where the two surfaces (at $z = 0, D$) preferentially attract the same or different components of the mixture. As stated earlier, depending on the surface potentials, the equilibrium state is either CW or PW [29].

Das *et al* have obtained a quantitative understanding of the pathways of segregation in both the diffusive and hydrodynamic cases. Here, we only show representative results from their studies. Figure 6 shows evolution pictures from a disordered

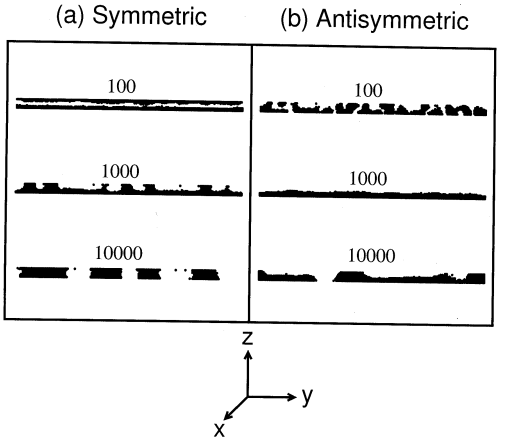

Figure 6. Phase-separation kinetics in $d = 3$ thin films of thickness $D = 10$. The simulation details (apart from the potential) are the same as for figure 1, and the system size is $512^2 \times 10$. (**a**) Evolution for the symmetric case with potential $V(z) = -0.1[(z+1)^{-3} + (D+1-z)^{-3}], z \in [0, D]$. (**b**) Evolution for the antisymmetric case with $V(z) = -0.05[(z+1)^{-3} - (D+1-z)^{-3}]$.

initial condition in the diffusive case. The parameters are chosen so that the surfaces are PW in equilibrium. The frames on the LHS show a symmetric film with $D = 10$. The equilibrium state is PW, but the rapid kinetics of surface enrichment results in a metastable CW state. This metastable state can be long-lived, depending on the proximity to the PW/CW line in the phase diagram. The CW state is finally broken up by fluctuations, and coarsening proceeds by the lateral diffusion of symmetric plugs. The frames on the RHS show the corresponding evolution for an antisymmetric film with $D = 10$. In this case, the coarsening plugs are cone-shaped due to the different contact angles on the two surfaces.

5. Conclusion

We conclude this paper with a brief summary and discussion of the results presented here. The presence of wetting surfaces has a strong effect on phase-separating binary mixtures. In particular, the interplay of wetting and segregation kinetics gives rise to a diverse range of novel and technologically relevant phenomena. This problem is usually referred to as *surface-directed spinodal decomposition* (SDSD).

In this paper, we have reviewed modeling and results for SDSD. We first focus on the case of a *semi-infinite geometry*, and clarify the kinetics of wetting-layer growth for arbitrary surface potentials and mixture compositions. The model for the semi-infinite system is readily adapted to the case of a *confined geometry*. Novel dynamical effects arise in confined systems due to the interaction of SDSD waves originating from different surfaces. Due to paucity of space, we have focused on specific features of SDSD here. However, there are many fascinating aspects of this problem, and it continues to be of great experimental and theoretical interest.

Acknowledgments

The authors are grateful to their coworkers for frutiful collaborations on the problems discussed here, in particular H L Frisch, B Aichmayer, S Bastea, S K Das, P Fratzl, J Horbach, J L Lebowitz, P Nielaba and G Saller.

References

[1] A J Bray, *Adv. Phys.* **43**, 357 (1994)
[2] K Binder and P Fratzl, in *Phase transformations in materials* edited by G Kostorz, (Wiley-VCH, Weinheim, 2001) p. 409
[3] S Dattagupta and S Puri, *Dissipative phenomena in condensed matter: Some applications* (Springer-Verlag, Heidelberg, 2004)
[4] R A L Jones, L J Norton, E J Kramer, F S Bates and P Wiltzius, *Phys. Rev. Lett.* **66**, 1326 (1991)
[5] G Krausch, *Mat. Sc. Engng Rep.* **R14**, 1 (1995)
[6] S Puri and H L Frisch, *J. Phys. Condens. Matter* **9**, 2109 (1997)
[7] K Binder, *J. Non-Equilib. Thermodyn.* **23**, 1 (1998)
[8] See Chapter 5 of ref. [3]
[9] K Binder, in *Phase transitions and critical phenomena* edited by C Domb and J L Lebowitz (Academic Press, London, 1983) vol. 8, p. 1
[10] S Dietrich, in *Phase transitions and critical phenomena* edited by C Domb and J L Lebowitz (Academic Press, London, 1988) vol. 12, p. 1
[11] P G de Gennes, *Rev. Mod. Phys.* **57**, 827 (1985)
[12] H W Diehl, in *Phase transitions and critical phenomena* edited by C Domb and J L Lebowitz (Academic Press, London, 1986) vol. 10, p. 75
[13] K Binder and H L Frisch, *Z. Phys.* **B84**, 403 (1991)
[14] S Puri and K Binder, *Phys. Rev.* **A46**, R4487 (1992); *Phys. Rev.* **E49**, 5359 (1994)
[15] P C Hohenberg and B I Halperin, *Rev. Mod. Phys.* **49**, 435 (1977)
[16] I Schmidt and K Binder, *Z. Phys.* **B67**, 369 (1987)
[17] S Puri and K Binder, *Z. Phys.* **B86**, 263 (1992)
[18] S Bastea, S Puri and J L Lebowitz, *Phys. Rev.* **E63**, 041513 (2001)
[19] H Tanaka, *J. Phys. Condens. Matter* **13**, 4637 (2001)
[20] S Puri and K Binder, *Phys. Rev. Lett.* **86**, 1797 (2001); *Phys. Rev.* **E66**, 061602 (2002)
[21] S Puri, K Binder and H L Frisch, *Phys. Rev.* **E56**, 6991 (1997)
[22] I E Dzyaloshinskii, E M Lifshitz and L P Pitaevskii, *Adv. Phys.* **10**, 165 (1961)
[23] Y Oono and S Puri, *Phys. Rev. Lett.* **58**, 836 (1987); *Phys. Rev.* **A38**, 434 (1988)
S Puri and Y Oono, *Phys. Rev.* **A38**, 1542 (1988)
[24] R Lipowsky and D A Huse, *Phys. Rev. Lett.* **57**, 353 (1986)
[25] S Puri and H L Frisch, *J. Chem. Phys.* **79**, 5560 (1993)
H L Frisch, S Puri and P Nielaba, *J. Chem. Phys.* **110**, 10514 (1999)
[26] S Puri and K Binder, *J. Stat. Phys.* **77**, 145 (1994)
[27] B Aichmayer, P Fratzl, S Puri and G Saller, *Phys. Rev. Lett.* **91**, 015701 (2003)
[28] S K Das, S Puri, J Horbach and K Binder, in preparation
[29] A J Liu, D J Durian, E Herbolzheimer and S A Safran, *Phys. Rev. Lett.* **65**, 1897 (1990)
L Monette, A J Liu and G S Grest, *Phys Rev.* **A46**, 7664 (1992)